HEAT AND MASS TRANSFER ENHANCEMENT STRATEGIES BY IMPINGING JETS
A Literature Review

by

Florin BODE[a,b], Claudiu PATRASCU[c], and Ilinca NASTASE[b*]

[a] Department of Mechanical Engineering, Technical University of Cluj-Napoca, Cluj-Napoca, Romania
[b] CAMBI Research Centre, Technical University of Civil Engineering, Bucharest, Romania
[c] Hydraulics Department, University Politehnica of Bucharest, Bucharest, Romania

Reviev paper
https://doi.org/10.2298/TSCI200713227B

Heat and mass transfer can be greatly increased when using impinging jets, regardless the application. The reason behind this is the complex behavior of the impinging jet flow which is leading to the generation of a multitude of flow phenomena, like: large-scale structures, small scale turbulent mixing, large curvature involving strong normal stresses, and strong shear, stagnation, separation, and re-attachment of the wall boundary-layers, increased heat transfer at the impinged plate. All these listed phenomena have highly unsteady nature and even though a lot of scientific studies have approached this subject, the impinging jet is not fully understood due to the difficulties of carrying out detailed experimental and numerically investigations. Nevertheless, for heat transfer enhancement in impinging jet applications, both passive and active strategies are employed. The effect of nozzle geometry and the impinging surface macro-structure modification are some of the most prominent passive strategies. On the other side, the most used active strategies utilize acoustical and mechanical oscillations in the exit plane of the flow, which in certain situations favors mixing enhancement. This is favored by the intensification of some instabilities and by the onset of large scale vortices with important levels of energy.

Key words: *impinging flow, heat transfer enhancement, electro-diffusion method, passive control, active control*

Introduction

By using impinging jets, the heat and mass transfer can be greatly increased, regardless the application. It is very well known that impinging jets are generating very high heat and mass transfer rates because they present among the most important heat and mass transfer rates, in particular if we refer to small values of the distance between the nozzle and the impinging plate [1, 2]. The main reason is that a surface-oriented jet can exchange significant rates of heat and mass between the impinging fluid and that plate. If we take, for example, the case of conventional convective cooling using a jet that is parallel to the target surface (heated or cooled), when using an impinging jet will lead to the increase of the heat transfer coefficients up to three times for the same flow rate. Engineering applications where impacting jets

* Corresponding author, e-mail: ilinca.nastase@utcb.ro

have found successful use belong to the following areas: furnace heating by the use of impinging flame jets [3], electronic components cooling [4], microelectronic industry [5], tempering of glass and metal sheets [6, 7], cooling of turbine blades [8], drying in textile and paper industry [9], air forced convection drying [10], cooling and heating in food industry [11], and many others. For example, in electronic industry, technological advancement is very much based on the capability to remove extremely large thermal loads from small surfaces [12]. In view of all this, the interest for the present subject, from the point of view of the theoretical and technical evaluations, continues to be doubtful.

In recent years, both experimental and numerical investigation tools and techniques have undergone exponential developments that allow for a deeper understanding of the phenomena involved in the impinging jets. Various review articles have approached the subject of heat and mass transfer in impinging jets beginning with [13] and continuing later with [14-18].

In the case of the impinging jets, turbulence varies significantly with nozzle geometry, upstream conditions and the distance between nozzle and impact plate [19].

The nozzle geometry and the upstream conditions are very important in designing heat transfer equipment for the case of low nozzle-to-plate distance H/D_e, but are less important if the impingement distance is higher than 8 ($H/D_e > 8$) [20].

Our understanding of the complex entanglement between fluid-flow and heat and mass transfer in any unsteady configuration it's in its adolescence, therefor the studies of impinging jets may offer a path towards fundamental knowledge of the subsequent phenomena.

Physics of the impinging jets

The most common nozzle orifices used for impinging jets in nowadays applications are either circular orifices or slit diffusers. The differences between these orifices is that in the first case the jet has an axisymmetric velocity profile and for the latter, the jet is wide and thin, having a plane 2-D velocity profile. These two types of jets have been studied extensively in reference articles both in the case of free jets [21, 22] and for impinging jets [23-25].

A typical axisymmetric impinging jet on a flat plate is shown in fig. 1. In this representation a uniform velocity jet is emerging from a circular nozzle and is impinging in a flat plate. Depending on the distance between the tip of the nozzle and the impinging jet, H, a maximum of four characteristic regions can be differentiated: a transition zone, a deceleration zone in the axial direction, a deflection zone and a zone with the flow in the radial direction.

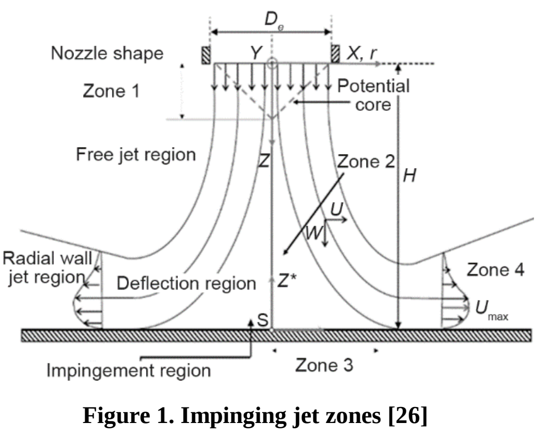

Figure 1. Impinging jet zones [26]

As stated in [22] the mean and turbulent velocity and temperature profiles issued from a nozzle orifice depends both on nozzle geometry shape and upstream flow conditions. For example, if the nozzle orifice is a pipe shaped nozzle, the flow will evolve into a velocity profile common for pipe flows and the turbulence of the flow will depend on the upstream flow conditions. In the case of a flow produced by a differential pressure on both sides of a thin plate with a circular orifice, in the immediate proximity downstream the orifice the phenomenon of *vena* *contracta* will appear. This flow particularity is that the flow through the orifice is forming a flat velocity profile with low turbulence intensity.

In the first region of the impinging jet, transition region, where the jet is sufficiently far away from the impinging plate, the jet will act as free submerged jet. This region is characterized by a spread of the flow starting from the exit of the nozzle orifice. This first region can be divided in three distinct subregions, fig. 1: potential core, settlement region, and fully established flow region.

In the potential core subregion where the jet is entering in the surrounding fluid, a potential cone flow, fig. 1, will be generated due to the appearance of a mixing annular shape region of increasing thickness. In the cone flow, given the fact that the jet is not mixing with the surrounding fluid, the fluid parameters are the same as in the nozzle region (temperature, velocity, concentration, *etc.*). Potential core (potential cone) is contained by the cone type region bounded by the condition of axial longitudinal mean velocity, U, of $0.99V_0$ (V_0 is the axial longitudinal velocity in the nozzle orifice). In the case of circular orifice nozzle the length of the potential core, fig. 1, varies around 4 to 6 nozzle diameters, D_e, [22, 27, 28].

Outside the potential core, in the mixing annular region we can find a very strong shear. Opposite from the potential cone, in the mixing annular region, the velocity will continue to decrease until it will reach the velocity of the surrounding fluid. This is possible by due to the fact that the fluid velocity of the potential core will decelerate by momentum exchange through the entrainment of the surrounding fluid by the fluid issued from the nozzle jet [22]. In this region, the turbulent energy originates from the symmetry line of the mixing layer where steeper velocity gradients occur. Here, eddies are found on the symmetry line of the mixing layer and their dimension is increasing with the distance from the nozzle orifice, Z. In the region next to the exit plane, these vortices appear to be coherent both in space and in time [29]. Also, in this area, the mean axial velocity and its turbulent component comply to similitude laws [21, 22, 30].

In the second region of the impinging jet, the deceleration zone, the axial velocity drops rapidly due to the proximity of the impinging plate, which effect will be maximum in the stagnation subregion where will force the flow to sudden change the direction.

This is known as the deflection zone, the third region of the impinging jet. In this region, in the proximity of the S point, fig. 1, impinging point, the flow will expand in radial directions parallel with the impinging plate. The S point is located at the intersection of the jet axis with the impinging plate and is also called stagnation point due to its zero velocity. The stagnation region is characterized by a high static pressure. The longitudinal component of the velocity decreases with the increase of the radial component of the velocity.

The fourth region of the impinging jet starts downstream the stagnation region, where the flow will spread in the radial direction towards the periphery of the plate, almost parallel to the wall and expands into a semi-confined flow. In this region, the flow has a finite width and due to the momentum exchange with the surrounding fluid, it evolves into a wall jet flow [31, 32].

In the case when impinging plate is located closer the nozzle orifice, some of the fourth regions cease to exist. The first region which disappear when the distance between the plate and the nozzle decrease is the jet fully developed region and after that, the decaying jet region will vanish. In the case of an impinging plate situated at $2D_e$ or less from the nozzle orifice, the high value of static pressure from the stagnation region will have a strong impact on the flow development from the nozzle orifice. Since the jet does not have enough distance to develop, the velocity profile is essentially uniform for the entire jet.

When studying impinging jets, two non-dimensional similitude criteria arise, Reynolds and Strouhal numbers:

$$\mathrm{Re}=\frac{\rho V D_e}{\eta}, \quad \mathrm{St}=\frac{f D_e}{V} \tag{1}$$

where ρ is the density of the fluid, η – the dynamic viscosity, V – the characteristic reference velocity, and f – the characteristic frequency.

If Reynolds number is the general approach of classifying flow behavior, Strouhal number describes the presence of pulsatile flow, such as vortex sheading.

Depending on the value of the Reynolds number the flow can be classified into four characteristic ranges: dissipated laminar jet for Re < 300, fully laminar when 300 < Re < 1000, transitional for 1000 < Re < 3000, and fully turbulent for Re > 3000.

Another source of turbulence, besides the generation that occurs in the jet flow field, is the shear flow region located at the jet edges which can induce instabilities somewhat similar to Kelvin-Helmholtz instability.

An analytical solution of the governing equations for the impinging jet can be obtained in the case of a system with axial symmetry and where the flow is in its laminar state. The momentum equation has to be coupled with the continuity equation. Also, if heat transfer is implied the energy equation must be coupled to. For such flow configurations, conservation of momentum, the continuity equation and the energy equation have following form:

$$\rho(v\partial_r v + u\partial_z v) = -d_r p + \partial_z(\eta\,\partial_z v) \tag{2}$$

$$\partial_r(\rho r v) + \partial_z(\rho r u) = 0 \tag{3}$$

$$\rho c_p(v\partial_r T + u\partial_z T) = \partial_z(k\,\partial_z T) \tag{4}$$

where ∂_r and ∂_z refers to the partial derivative with respect to r and z, respectively, and c_p is the specific heat of the fluid at constant pressure.

All three equations must be solved with the appropriate boundary conditions: for $z = 0$:$u = 0$, $T = T_\mathrm{w}$, and for $z \to \infty$:$u = 0$, $v = V_\mathrm{s}$, $T = T_\infty$.

In general, solutions of these equations are found in terms of similarity solutions. Sibulkin [33] found a solution to the energy equation in Zone 3 by defining a dimensionless temperature function as $f(\zeta)=(T-T_\infty)/(T_w-T_\infty)$. The dimensionless expression of eq. (4) then becomes:

$$f'' + 2f\,\mathrm{Pr}\,f' = 0 \tag{5}$$

where $\mathrm{Pr} = \eta c_p/k$ is Prandtl number and $\zeta=\sqrt{a\eta/\rho z}$, if one considers that the velocity at stagnation point is $V_\mathrm{s} = ar$.

The solution of eq. (5) is then found to be:

$$\frac{\mathrm{Nu}}{\sqrt{\mathrm{Re}}} = 0.763\,(a^*)^{0.5}\,\mathrm{Pr}^{0.4} \tag{6}$$

where a^* is a free constant that depends on the geometry of the system.

In Zone 4, Glauert [34] finds a solution by introducing a friction coefficient as a function of the Reynolds number:

$$\frac{\mathrm{Nu}}{\mathrm{Re}\sqrt[3]{\mathrm{Pr}}} = \frac{c_\mathrm{f}}{2} \tag{7}$$

If this friction coefficient is known, then the local and average heat transfer coefficients can be determined.

Two important parameters that quantify heat transfer are the convective heat flux, q_c, which represents the thermal energy transfer per unit surface and per unit time, and the convective heat transfer coefficient, h, representing heat per unit temperature difference. The relation between the latter two in the steady state is referred to as Newton's law:

$$q_\mathrm{c} = h(T_\mathrm{w} - T_\mathrm{aw}) \tag{8}$$

where T_w is the temperature of the surface and T_aw – a reference value for temperature called adiabatic wall temperature.

Combining eq. (1) with the Fourier law, the heat transfer coefficient has the following form:

$$h = \frac{-k\left(\dfrac{\mathrm{d}T}{\mathrm{d}z}\right)_\mathrm{w}}{(T_\mathrm{w} - T_\mathrm{aw})} \tag{9}$$

where k is the thermal conductivity coefficient of the fluid specified by the wall conditions.

Convective heat transfer and mass transfer are usually quantified by non-dimensional quantities such as the Nusselt and Sherwood number, respectively. Their expressions are given by the following relations:

$$\mathrm{Nu} = \frac{hD_e}{k}, \quad \mathrm{Sh} = \frac{\beta D_e}{\delta} \tag{10}$$

where D_e is the characteristic flow length, β – the mass transfer coefficient, and δ – the diffusion coefficient.

Both parameters are a function of the fluid flow geometry and the Reynolds number.

When the initial temperature of the jet is equal to the one of the ambient medium an important parameter is the recovery factor, a parameter proportional to the difference between the recovery temperature, T_r, and the static temperature at the nozzle exit:

$$r_\mathrm{f} = \frac{2c_p(T_\mathrm{r} - T)}{V^2} \tag{11}$$

Passive strategies for heat transfer enhancement

Some of the most important mechanisms that influence the mass and heat transfer of the impinging jet are the instability of the shear layer in the proximity of the exit plane of the nozzle and the onset of turbulence in the jet near field. In the case of 2-D jet impinging in a flat plate [35], the increased heat transfer can be explicated as a result of the higher turbulence generated in the impinging jets. They found [35] that the turbulence originates from the flow itself and from external perturbances and is influenced greatly by the nozzle orifice geometry, the upstream flow conditions and the position within the jet.

The effect of nozzle design

The most common passive strategies are based on the nozzle orifice geometry [36-40]. The research carried out showed that particularities of the nozzle geometry and of the upstream flow setup, are of great importance in designing of heat transfer devices where we have low nozzle to plate distance $H/D_e < 8$, but are less important if nozzle to plate distance is more than $H/D_e > 8$.

The geometries of nozzles and diffusers became more and more complex in the quest of best geometries capable to enhance the self-induction of the non-symmetric large scale structures [41-44]. Research carried out on rectangular nozzles showed the appearance of an interesting phenomenon of the switch between the major and minor axis of this rectangular jet. In [45], the researchers identified a linear dependence between nozzle aspect ratio and the length from the orifice to the first cross-over location. Afterwards, Quinn [46] discovered the pairs of counter revolving streamwise vortices at the tips of rectangular nozzles and showed that these structures have an important role in the momentum transport. In the meantime, a study performed on elliptic jets by Hussain and Husain [42] revealed that, unlike circular or plane type of jets, these jets have a variation of vortical structures azimuthal curvature. This will lead to an unbalanced self-induction which will evolve in axis switching.

These researches opened the way to other approaches in a quest for improving jet flows spreading and mixing only by nozzle design. For example, in the case of rectangular and circular tabbed nozzles researches revealed a higher mixing efficiency than the same rectangular or circular nozzles without tab intrusions [44, 47-49]. The explanation was that each tab introduce a pair of counter rotating streamwise vortices which changes the turbulent structure and is leading to an enhancement mixing in the flow.

More complex nozzle geometries have been studied [50, 51], one of the conclusions emerged from [52-54] being that the lobed nozzle performed better in mixing than other similar nozzles.

The conclusions emerged from the studies have been take into consideration for impinging jet studies, as well. Brignoni and Garimella [55] showed that the heat transfer will increase with 20-30% in the case of nozzles with chamfered outlets compared with non-chamfered ones. Different elliptic nozzles are compared with a circular one in [56], a conclusion being that the heat transfer is with 15% larger for an elliptic nozzle orifice nozzle with the aspect ratio equal to 4 than for the circular nozzle.

Other researches have oriented in the direction of creating of vortices and turbulence generators with the nozzle geometry design. For the case of chevron nozzle – triangular tabs placed in a circular orifice – an enhancement higher than 25% compared to the round orifice was observed for $4D_e$ nozzle to impinging wall distance [57]. Also, the flow through the cross-shaped lobed nozzle achieved the highest heat transfer compared with circular nozzle orifice [19, 58, 59]. A fractal-shaped design was used for heat transfer enhancement for impingement cooling in [60].

Lobed nozzles orifices were found to increase both wall shear rate and local or global mass transfer, suggesting a relation between the latter two. The maximum local Sherwood number can get up to 130% higher for a cross-shaped orifice on a plane or on a hemisphere compared to the convergent nozzle orifice. The evaluation of the global mass transfer is obtained using the average Sherwood number, which for a disc of $3.2D_e$ in diameter reveals an improvement up to 25 and 22% for cross-shaped orifice on a plane or on a hemisphere, respectively, compared to a convergent nozzle. The study of a cross-shaped orifice on a hemisphere nozzle geometry showed an increase for local and global mass transfer [61].

Compared to a convergent nozzle, the instantaneous velocity fields issued from a round orifice from a flat plate or a hemispherical geometry, show the formation of secondary vortices above the impingement plate, under primary Kelvin-Helmholtz structures in the region $r = 1.5\ D_e$. From $r = 1.5\ D_e$, the structures generated by the breaking of the primary Kelvin-Helmholtz structures are getting further away from the wall. Considering constant volumetric flow rate and the same nozzle exit area, the global mass transfer for one impinging disk of $3.2D_e$ in diameter is 25% and 31%, respectively, higher for a round orifice nozzle on a hemispherical or on a plane surface compared to the classical convergent nozzle. Regarding local mass transfer, local Sherwood number distributions (as a function of the normalized radial distance from the stagnation point) indicate an increase of 19% and 34% for the same compared nozzle geometries, fig. 2.

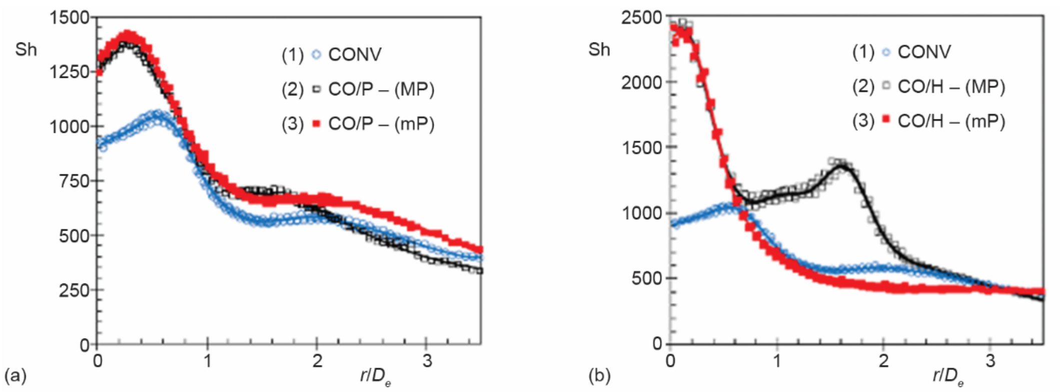

Figure 2. Sherwood number for: (a) convergent nozzle (CONV) and cross-shaped nozzle orifice on a plate, CO/P and (b) convergent nozzle (CONV) and cross-shaped nozzle orifice on a hemisphere, CO/H [62]

These distributions also point out a secondary peak at the wall region where secondary vortices appear, the magnitude of this secondary peak being dependent on nozzle shape. Increasing inertia results in an increase of the magnitude of the secondary peak [63, 64]. Jets from lobed nozzles display particular phenomena due to the complexity of their 3-D flow, as reported by Trinh *et al.* [65]. They recorded the presence of two shear layers one spanning from the central part to the lobed flow and the other from the lobed flow to the environment, both merging one or two diameters away from the nozzle. They also found that for $h/D_e \leq 2$ the nozzle has a significant influence on the flow, causing multiple mean radial velocity maxima, flow in the azimuthal direction and recirculation zones near the plate. Such lobed nozzles have the tendency to decrease the global heat transfer rate.

Regarding the movement of the impingement region, recent studies have been employed in evaluating its dependence on the flow rate, the nozzle geometry and the nozzle height [66]. It was found that the movement of the impingement region can be linearly correlated with the stand-off height. Compared to a flat nozzle a conical-shaped nozzle slightly reduced the movement, the external geometry having therefor a small effect. No dependence was found on the flow rate.

The major effect of a non-quiescent external medium on the dynamics and turbulent behavior of a plane jet impinging on a flat plate is a reduction of the jet decay rate compared to an external flow at rest [67]. Such co-flow configurations exhibit an increase in radial turbulence of the impinging jet. For inclination angles of the co-flow higher than 30° a large recirculation zone is induced [67].

Surface structure modification

Hansen and Webb [68] showed that for impinging surface with protuberances representing triangular, square or rectangular cross section shapes, Nusselt number will increase with 12-23% than for a flat plate. A heat transfer growth of 8-28% will appear for cube shape surface roughness [69]. On the other hand, the heat transfer coefficient for a dimpled surface is lower than for a smooth surface [70]. In other studies [71, 72], the impinging slot jets oriented over square and triangular ribbed surface were reported to have an increase in heat transfer compared to a plane surface. The reason can be the interaction of two factors, namely: the increased mixing induced by the turbulence generated by the ribs and the increased area for the heat transfer surfaces due to the ribs themselves. Other ribbed surfaces as equilateral triangles which are basically vortices generators were analyzed in [73], and the conclusion was that the convective heat coefficient between the impinging flow and the wall is linked to the aspect of the rib. Heat transfer coefficient enhancement was up to 77%.

Some studies were focused on the modifications in the heat transfer brought by enhanced surfaces in spray cooling. One of the firsts attempts made, using structured surfaces as a method to increase heat flux is found in [59]. Using water as a fluid, they modified a copper surface and obtained a roughness ranging from 0.3-22 μm. They achieved a maximum heat flux of 1250 W/cm^2 for a roughness of 0.3 μm and 700 W/cm^2 for 22 μm, at a flow rate of 1.42 mL/s of water and 250 mL/s of air. A heat transfer coefficient higher with 112% was obtained by Bostanci *et al.* [74] using ammonia as a working fluid and structure surfaces using RTI as a surface modification technique [74].

The effect of a macro-structured surface on the enhancement of heat flux was emphasized by Silk *et al.* [75]. Using protuberances like fins, pins and pyramids, constructed on a 2 cm^2 surface, working at a pressure of 41.4 kPa and at a flow rate of 3.33 mL per second, they found that straight fins display the best performance. They achieved a heat flux enhancement of 75% for a surface with straight fins and a spray nozzle inclined at 45°. Not only the geometry but also its characteristic height has a significant importance. For example, Coursey *et al.* [76] considered straight fin structures on surfaces with fin heights ranging from 0.25-5 mm. At a flow rate of 1 mL per second, the optimal fin height that ensured the maximum heat flux of 124 W/cm^2, was found between 1 and 3 mm. Coating a surface may ultimately lead to the enhancement of heat transfer [77]. Investigating micro-porous coated surfaces, in the context of spray cooling enhancement, they found an increase of 50% relative to the uncoated ones for a microporous layer of 500 μm thick and consisted of micro-sized aluminium particles. Xie [78] studied the effects of micro-, macro- and multiscale-structured surfaces. For a macro-structured surface the fin arrangement is a key aspect of heat transfer enhancement, in comparison with an increase of the wetted area. The advantage of macro-structured surfaces is that it reduces the duration of the high temperature regime and has an increasing effect on the transition time needed to reach the critical heat flux moment. In the case of micro-structured shapes, an enhancement of nucleate boiling was notices. The largest heat transfer increasing was achieved by using the multiscale-structured geometries which was of 65% in comparison with a flat baseline. In another study, El-Maghlany *et al.* [79] discovered that the for the two ribs mounted on a horizontal flat surface, heat transfer rate will be influenced by the distance between the ribs and the rib height. Also, the heat transfer rate increased with the nanoparticles volume fraction.

Active strategies in heat transfer

The active strategies methods uses mainly the acoustic [42-44, 80-82] or mechanical [83-88] excitation in nozzle orifice area, which under some particular conditions will lead to the intensification of the initial instabilities and the occurrence of large scale, very energetic, vortex structures that are responsible for the mixing improvement.

A study [89] investigated the effect of active strategies on the impinging jet using flow visualization and velocity spectra through hot wire anemometry. Depending of the growth in dimensions of the large scale vortices occuring in the wall jet region, both heat transfer increasing, and reduction are observed. For a frequency of excitation close to the natural frequency of the shear layer in the initial region of the impinging flow, the induced intermittent vortex pairing produces a chaotic bump eddy which contains much of the small-scale turbulent structures, leading to the increase in the local heat transfer. When the forcing is near the sub-harmonic of the natural frequency, stable vortex pairing is generated. In this case the strong large-scale well-organized vortices, formed after the stable vortex pairing, induce the unsteady separation of the wall boundary layer leading to a decrease in the local heat transfer.

Acoustic excitation also offers a way of controlling vortex interaction [90, 91]. A shorter potential core length and an increase of the turbulent intensity is observed relative to non-excited jets for St = 1.2. As the turbulent intensity increases also the heat transfer rate is enhanced for small H/D_e ratios. The suppression of vortex pairing arises when St = 2.4. This results in a large potential core length and a reduced turbulent intensity. Not only the frequency of the excitation but also the signal shape can cause heat transfer deterioration. For example, Middelberg and Herwig [92] studied several signal shapes at different driving frequencies and found that at the highest Strouhal number both sinusoidal and rectangular signals caused an enhancement in heat transfer of 60% in the stagnation zone and up to 160% outside of it. The high levels of enhancement are caused by periodic flow reversal, which has also an effect on the ambient fluid, coffining it to participate in heat transfer. More on the relation between periodic flow reversal, resonance in the flow path and compressibility can be found in [93, 94]. The experimental results of a free impinging jet seeded with a high concentration of SiO_2 nanoparticles presented by Sorour *et al.* [95] show that the increase of the volumetric fraction of nanoparticles and of the Reynolds number will conduct to an increase oftric the average Nusselt number. As a consequence, the volume fraction of nanoparticles could significantly provide an increase of the average Nusselt number up to 80% for a volume fraction of 8.5% SiO_2 nanoparticles compared to a water jet flow without nanoparticles. Lai *et al.* [96], studied impulsively starting jets and pulsed jets for heat transfer enhancement.

Advanced experimental techniques and perspectives

Impinging jets are responsible for generation of a multitude of flow phenomena, such as: large scale structures, large curvature involving strong normal stresses and strong shear, small scale turbulent mixing, stagnation, separation, and re-attachment of the wall boundary layers, heat transfer at the impinged wall. All these phenomena have a large degree of unsteadiness and although there are many studies today on this subject that tried to resolve this subject, the impinging jets are still not fully understood due to their unsteady nature and due to the difficulty of performing elaborated numerical and experimental studies [76].

One of the most promising measurement techniques of the mass transfer between an impinging jet and the impinging plate is the limiting diffusion current technique. In [97], a circular disk electrode localized in the impinging plate, in the zone of stagnation, was used for this technique. The authors discovered that if for a turbulent impinging jet the electrode location corresponds with a radius smaller than $1D_e$, or if the impinging jet is laminar, the electrode displays the property of *uniform accessibility* to the diffusing species. They determined semi empirical correlations for both laminar and turbulent impinging jets in a plate for nozzle-to-plate distances from $0.2D_e$ to $6D_e$. Another observation was related with the wall jet region which is beginning at a radial length of ~$4D_e$.

Another promising measurement technique, this time for measurement of the fluid flow is particle image velocimetry (PIV). Having in mind that the impinging jet has a 3-D nature due to the nozzle design or impinging plane structure, only latest advancement in the PIV technique like tomographic PIV (TomoPIV) allows a 3-D appropriate approach for the fluid flow analysis. The main difference between classical PIV and TomoPIV is that instead of generating a double-pulsed laser sheet illumination of a plane in the measurement zone, a double-pulsed laser illumination of a volume will be created. For both approaches the fluid-flow is seeded with particles but in the case of TomoPIV the particle distribution is determined using multiple camera (at least three), which will allow to obtain the volumetric velocity distribution through a cross-correlation algorithm in the entire volume. This way, the calculation of derivative quantities becomes possible, offering the possibility of a detailed picture of vortex dynamics and turbulence characteristics [98]. A drawback of the PIV technique is the fact that the measurements performed in the close vicinity of the impinging plate are not possible and reliable due to the laser light reflections from the impinging plate.

In its turn, the electro-diffusion (ED) method whose measurement principle is related to the recording of the limiting diffusion current of an electrode-type probe [99] seems to be the best technique for determining the shear rate at the impinging wall [100]. The ED technique was developed with the purpose of measuring the mean values of the mass transfer rate on a wall. The transfer area is represented by a small electrode embedded into the wall, at the same level as the surface of the wall. An electrochemical redox reaction occurs at the electrode, the mass transfer influencing directly its rate. Vallis *et al.* [101] published the first results using ED measurements technique in 1977. Later, Yapici *et al.* [102] succeed to measure the distributions of the local shear stress on the entire impinging plate for a fully developed round turbulent submerged jet. They found that the non-dimensional local shear stresses diminished with the growth of the Reynolds number. In other study [103] the authors measured the influence of the axial velocity on the electrode currents of a circular probe with three segments in the proximity of the stagnation point. Their flow was characterized by a Reynolds number Re = 640 while Alekseenko *et al.* [104] measured wall shear stresses of a circular impinging jet at Re = 41600 and for nozzle-to-plate distances from 2 to $8D_e$. Considering the observations related with the flow dynamic of lobed orifice free jet which is characterized by amplified dynamics of the coherent and non-coherent structures and intensified turbulent kinetic energy in its initial region, it was considered that the jet flow will also present increased mass transfer for impinging jet cases.

Kristiawan *et al.* [19] studied comparatively a cross-shaped nozzle and a convergent circular nozzle with the same D_e in terms of mass transfer rates. The insight gained in a previous study [105] of a cross-shaped orifice air free jet is used to get knowledge for the aforementioned two impinging jets. The wall shear rate was measured by ED technique on an impinging plate and mass transfer was calculated using these measurements. Different results for the wall shear rate and for the mass transfer at the stagnation point were attained using the cross shaped lobed nozzle flow compared with the circular convergent nozzle. First time when using simultaneously time resolved PIV and ED measurements in an attempt to resolve both the fluid-flow and wall shear rate [106, 107] they observed that the influence of the between primary on the secondary vortices, and their pairing process, and their interaction with tertiary prior upstream structures, affects the process of structures expulsion near the wall and afterwards the wall shear stress value. Sodjavi *et al.* [108] performed experimental measurements involving non-synchronized time resolved TomoPIV and ED technique on the flow issued through three circular nozzle orifices: an orifice plate, a convergent and a hemispherical one. With this occasion the authors presented a possible connection between the wall shear stress and the mass transfer rate with the topology of the near field. The velocity instantaneous fields obtained through PIV showed the generation of secondary structures in the area where a secondary peak of the evolution of the local mass transfer rate appears and more than that, the intensity of this secondary peak was corelated with the nozzle orifice design.

Conclusions

Heat and mass transfer can be greatly increased when using impinging jets, regardless the application. It is very well known that impinging jets are generating very high heat and mass transfer rates because they present among the most important rates of transfer rate for single phase flows, especially if we refer to low nozzle-to-plate distances. The reason behind this is the complex behavior of the impinging jet flow which is leading to the generation of a multitude of flow phenomena, like: large scale vortices, high curvature related to high values of the normal stresses and intense shear rate, small scale turbulent mixing, stagnation, separation and re-attachment of the boundary-layers, increased heat transfer at the impinged surface. All these listed phenomena have highly unsteady nature and even though a lot of scientific studies have approached this subject, the impinging jet flows are not entirely comprehended due to the difficulties of carrying out thorough experimental and numerically investigations. To overcome these difficulties in order to gain insight about these phenomena, we must use procedures that are adapted to our objectives.

First step for impinging jet measurements is to realize measurements using TomoPIV technique which will grant a higher spatial resolution to capture the 3-D characteristics of the complex flow. The ED measurements must be synchronized with Tomo PIV measurements. More than that, 3-D laser Doppler velocimetry (LDV) measurements triggered by ED signal represents a very useful and complementary method that allows the investigation of targeted zones of interest in the flow. For example, LDV measurements of the velocity components in the vicinity of a modified surface with triangular ribs have been successfully engaged. Nevertheless, more knowledge is needed about the vortex dynamics and breakdown as well as on the influence of streamwise vorticity. These issues appeal for the perfecting of particular experimental techniques such as ED, IR thermography, and TomoPIV.

Advanced passive strategies like lobed orifice nozzle geometries or structured impinged surfaces are not sufficiently studied. All the aforementioned issues must be investigated not only experimentally but also numerically using CFD to gain further knowledge on this phenomenon of impinging jet given the fact that it takes less effort and time than experimental measurements. Nevertheless, performing real experiments it is irreplaceable because the development, perfecting, verification and validations of theories and models are still based on results issued from experiments and invites for more demanding measurement techniques.

Acknowledgment

This work was supported by a grant of the Romanian Ministry of Education and Research, CCCDI-UEFISCDI, project number PN-III-P2-2.1-PED-2019-4249, within PNCDI III, XTREME - Innovative system to extend the range of electric vehicles at improved thermal comfort

Nomenclature

c_p – specific heat of the fluid at constant pressure, [Jkg^{-1}K^{-1}]
D_e – characteristic flow length, [m]
f – characteristic frequency, [s^{-1}]
h – heat transfer coefficient, [Wm^{-2}K^{-1}]
H – nozzle to plate distance, [m]
k – thermal conductivity coefficient, [Wm^{-1}K^{-1}]
Nu – Nusselt number (= hD_e/k), [–]
Pr – Prandtl number (= $\eta c_p/k$), [–]
q_c – convective heat flux, [Wm^{-2}]
Re – Reynolds number (= $\rho VD_e/\eta$), [–]
Sh – Sherwood number (= $\beta D_e/\delta$), [–]
St – Strouhal number (= fD_e/V), [–]
T_{aw} – reference value for adiabatic wall temperature, [K]
T_w – temperature of the surface, [K]
V – velocity, [ms^{-1}]

Greek symbols

β – convective mass transfer coefficient, [ms^{-1}]
ρ – density of the fluid, [kgm^{-3}]
δ – diffusion coefficient, [m^{2}s^{-1}]
η – dynamic viscosity, [Pa·s]

Acronyms

MP – major plane
mP – minor plane

References

[1] Narayanan, V., *et al.*, An Experimental Study of Fluid Mechanics and Heat Transfer in an Impinging Slot Jet Flow, *International Journal of Heat and Mass Transfer, 47* (2004), 8-9, pp. 1827-1845
[2] Baydar, E., Ozmen, Y., An Experimental and Numerical Investigation on a Confined Impinging Air Jet at High Reynolds Numbers, *Applied Thermal Eng*., *25* (2005), 2-3, pp. 409-421
[3] Viskanta, R., Heat Transfer to Impinging Isothermal Gas and Flame Jets, *Experimental Thermal and Fluid Science, 6* (1993), 2, pp. 111-134
[4] Fabbri, M., *et al.*, A Comparative Study of Cooling of High Power Density Electronics Using Sprays and Microjets, *Journal of Heat Transfer, 127* (2005), 1, pp. 38-48
[5] Qiu, S. X., *et al.*, Enhanced Heat Transfer Characteristics of Conjugated Air Jet Impingement on a Finned Heat Sink, *Thermal Science, 21* (2017), 1, pp. 279-288
[6] Gardon, R., Akfirat, J. C., Heat Transfer Characteristics of Impinging Two-Dimensional Air Jets, *J. Heat Transfer, 88* (1966), 1, pp. 101-108
[7] Gardon, R., Cobonpue, J., Heat Transfer Between a Flat Plate and Jets of Air Impinging on It. *Proceedings,* 2nd Heat Transfer Conf., New York, USA, 1962, pp. 454-460
[8] Han, B., Goldstein, R. J., Jet-Impingement Heat Transfer in Gas Turbine Systems, *In Annals of The New York Academy Of Sciences, 934* (2001), 1, pp. 147-161
[9] Polat, S., Heat and Mass Transfer in Impingement Drying, *Drying Technology, 11* (1993), 6, pp. 1147-1176
[10] Alnak, D. E., Karabulut, K., Analysis of Heat and Mass Transfer of The Different Moist Object Geometries with Air Slot Jet Impinging for Forced Convection Drying, *Thermal Science,22* (2018), 6, pp. 2943-2953
[11] Sarkar, A., *et al.*, Fluid Flow and Heat Transfer in Air Jet Impingement in Food Processing, *Journal of Food Science, 69* (2004), 4, pp. CRH113-CRH122
[12] Anwarullah, M., *et al.*, Experimental Investigation for Enhancement of Heat Transfer From Cooling of Electronic Components by Circular Air Jet Impingement, *Heat and Mass Transfer, 48* (2012), 9, pp. 1627-1635

[13] Martin, H., Heat and Mass Transfer Between Impinging Gas Jets and Solid Surfaces, *Advances in Heat Transfer*, *13* (1977), pp. 1-60
[14] Carlomagno, G. M., Ianiro, A., Thermo-Fluid-Dynamics of Submerged Jets Impinging at Short Nozzle-To-Plate Distance: A Review. Exp, *Thermal and Fluid Science*, *58* (2014), Oct., pp. 15-35
[15] Hall, J. W., Ewing, D., On the Dynamics of the Large-Scale Structures in Round Impinging Jets, *Journal of Fluid Mechanics, 555* (2006), May, pp. 439-458
[16] Harmand, S., *et al.*, Review of Fluid Flow and Convective Heat Transfer Within Rotating Disk Cavities With Impinging Jet, *International Journal of Thermal Sciences, 67* (2013), May, pp. 1-30
[17] Polat, S., *et al.*, Numerical Flow and Heat Transfer Under Impinging Jets: A Review, *Annual Review of Numerical Fluid Mechanics and Heat Transfer, 2* (1989), pp. 157-197
[18] Nastase, I., Bode, F., Impinging Jets – A Short Review on Strategies for Heat Transfer Enhancement, E3S Web Conf., *32* (2018), Feb., 01013
[19] Kristiawan, M., *et al.*, Wall Shear Rates and Mass Transfer In Impinging Jets: Comparison of Circular Convergent and Cross-Shaped Orifice Nozzles, *International Journal of Heat and Mass Transfer, 55* (2012), 1-3, pp. 282-293
[20] Hammad, K. J., Milanovic, I., Flow Structure in the Near-Wall Region of a Submerged Impinging Jet, *Journal of Fluids Engineering-Transactions of the Asme, 133* (2011), 9, 091205
[21] Abramovich, G. N., *The Theory of Turbulent Jets*, MIT Press, Cambridge, Mass., USA, 1963, 668
[22] Rajaratnam, N., *Turbulent Jets*, Elsevier Scientific Publishing Company, Amsterdam, The Netherlands, 1976
[23] Martin, H., Heat and Mass Transfer Between Impinging Gas Jets and Solid Surfaces, *Advances Heat Transfer, 13* (1977), pp. 1-60
[24] Jambunathan, K., *et al.*, A Review of Heat Transfer Data for Single Circular Jet Impingement, *International Journal of Heat and Fluid Flow, 13* (1992), 2, pp. 106-115
[25] Carlomagno, G. M., Ianiro, A., Thermo-Fluid-Dynamics of Submerged Jets Impinging at Short Nozzle-To-Plate Distance: A Review, *Experimental Thermal and Fluid Science, 58* (2014), Suppl. C, pp. S15-S35
[26] Meslem, A., *et al.*, Flow Dynamics and Mass Transfer in Impinging Circular Jet at Low Reynolds Number, Comparison of Convergent and Orifice Nozzles, *International Journal of Heat and Mass Transfer, 67* (2013), Dec., pp. 25-45
[27] Awbi, H. B., *Ventilation of Buildings*, E&FN SPON, London, UK, 313, 1991
[28] Oosthuisen, P. H., An Experimental Study of low reynolds number turbulent circular jet flow. In asme Applied Mechanics, *Proceedings*, Bioengineering and Fluids Engineering Conference, Houston, Tex., USA, 1983
[29] Davies, P. A. O. L., *et al.*, The Caracteristics of the Turbulence in the Mixing Region of a Round Jet, *Journal of Fluid Mechanics, 15* (1963), 3, pp. 337-367
[30] Rajaratnam, N., Pani, B. S., Turbulent Compound Annular Shear Layers, *J. Hydraulics Division*, *98* (1972), 7, pp. 1101-1115
[31] Kristiawan, M., *et al.*, Mass Transfer and Shear Rate on a Wall Normal to an Impinging Circular Jet, *Chemical Engineering Science, 132* (2015), Aug., pp. 32-45
[32] Hassan, M., *et al.* , Experimental Investigation of the Wall Shear Stress and the Vortex Dynamics in a Circular Impinging Jet, *Exp Fluids*, *52* (2012), 6, pp. 1475-1489
[33] Sibulkin, M., Heat Transfer Near the Forward Stagnation Point of a Body of Revolution Journal of Aero, *Sciences, 9* (1952), pp. 570-571
[34] Glauert, M. B., The Wall Jet, *Journal of Fluid Mechanics*, *1* (1956), pp. 625-643
[35] Gardon, R., Akfirat, J. C., Heat Transfer Characteristics of Impinging Two-Dimensional Air Jets, *Journal of Heat Transfer, 88* (1966), 1, pp. 101-107
[36] Chaudhari, M., *et al.*, Effect of Orifice Shape in Synthetic Jet Based Impingement Cooling, *Experimental Thermal and Fluid Science, 34* (2010), 2, pp. 246-256
[37] Garimella, S. V., Nenaydykh, B., Nozzle-Geometry Effects In Liquid Jet Impingement Heat Transfer, *International Journal of Heat and Mass Transfer, 39* (1996), 14, pp. 2915-2923
[38] Pan, Y., *et al*., Webb, Effect of Nozzle Configuration on Transport in the Stagnation Zone of Axisymmetric, Impinging Free-Surface Liquid Jets, Part 2, Local heat transfer, *Journal of Heat Transfer, 114* (1992), 4, pp. 880-886
[39] Bode, F., *et al.*, Numerical Prediction of Wall Shear Rate in Impinging Cross-Shaped Jet at Moderate Reynolds Number, Scientific Bulletin of UPB, Series D: *Mech. Eng.*, *79* (2014), 12, pp. 251-258

[40] Bode, F., *et al.*, Flow and Wall Shear Rate Analysis for a Cruciform Jet Impacting on a Plate at Short Distance Progress in Computational Fluid Dynamics, *An Int. J., 20* (2020), 38
[41] Zaman, K. B. M. Q., Hussain, A. K. M. F., Vortex Pairing in a Circular Jet Under Controlled Excitation, Part 1, General Response, *Journal of Fluid Mechanics, 101* (1980), 3, pp. 441-491
[42] Hussain, F., Husain, H. S., Elliptic Jets, Part1, Characteristics of Unexcited and Excited Jets, *Journal of Fluid Mechanics, 208* (1989), Nov., pp. 257-320
[43] Lin, Y. T., *et al.*, Investigation on the Mass Entrainement of an Acoustically Controlled Elliptic Jet, *International Communications in Heat and Mass Transfer, 25* (1998), 3, pp. 379-388
[44] Zaman, K. B. M. Q., Axis Switching and Spreading of an Asymmetric Jet: The Role of Coherent Structure Dynamics, *Journal of Fluid Mechanics, 316* (1996), 1, pp. 1-27
[45] Krothapalli, A.,*et al.*, On The Mixing of a Rectangular Jet, *Journal of Fluid Mechanics, 107* (1981), June, pp. 201-220
[46] Quinn, W. R., Streamwise Evolution of a Square Jet Cross-Section, *AIAA Journal, 30* (1992), 12, pp. 2853-2857
[47] Zaman, K. B. M. Q., Spreading Characteristics and Thrust of Jets From Asymmetric Nozzles, AIAA Paper No 96-0200, 1996
[48] Hu, H., *et al.*, Changes to the Vortical and Turbulent Structure of Jet Flows Due to Mechanical Tabs., Proceedings, *Instn. Mech. Engrs., 213* (1999), Part C, pp. 321-329
[49] Hu, H., *et al.*, Passive Control on Jet Mixing Flows by Using Vortex Generators, *Proceedings*, 6th Triennial International Syposium on Fluid Control, Measurement and Visualisation, Sherbrooke, Canada, 2000
[50] Belovich, V. M., Samimy, M., Mixing Processes in a Coaxial Geometry with a Central Lobed Mixer-Nozzle, *AIAA Journal, 35* (1997), 5, pp. 838-841
[51] Yuan, Y., Jet Fluid Mixing Control Through Manipulation of Inviscid Flow Structures, Ph.D. Thesis, Virginia Polytechnic Institute and State University, Blacksbury, Va., USA. 2000
[52] Hu, H., *et al.*, Particle Image Velocimetry and Planar Laser Induced Fluorescence Measurements on Lobed Jet Mixing Flows, *Experiments in Fluids, 29* (2000), Suppl. 1, pp. S141-S157
[53] Hu, H., *et al.*, Research on the Vortical and Turbulent Structures in the Lobed jet Flow Using Laser Induced Fluorescence and Particle Image Velocimetry Techniques, *Measurement Science and Technology, 11* (2000), 6, pp. 698-711
[54] Hu, H., *et al.*, A Study on a Lobed Jet Mixing Flow by Using Stereoscopic Particle Image Velocimetry Technique, *Physics of Fluids, 13* (2001), 11, pp. 3425-3441
[55] Brignoni, L. A., Garimella, S. V., Effects of Nozzle-Inlet Chamfering on Pressure Drop and Heat Transfer in Confined Air Jet Impingement, *International Journal of Heat and Mass Transfer, 43* (2000), 7, pp. 1133-1139
[56] Lee, J., Lee, S. J., The Effect of Nozzle Aspect Ratio on Stagnation Region Heat Transfer Characteristics of Elliptic Impinging Jet, *International Journal of Heat and Mass Transfer, 43* (2000), 4, pp. 555-575
[57] Gao, N., *et al.,* Heat Transfer to Impinging Round Jets with Triangular Tabs., *International Journal of Heat and Mass Transfer, 46* (2003), 14, pp. 2557-2569
[58] Bode, F., A. *et al.*, Numerical Simulation of a Very Low Reynolds Cross-Shaped Jet, *Mechanics, 19* (2013), 5, pp. 512-517
[59] Bode, F., *et al.* Comparison of Turbulence Models in Simulating a Cruciform Impinging Jet on a Flat Wall, *Proceedings*, 14th International Heat Transfer Converence, Kyoto, Japan, 2014
[60] Cai, L., *et al.*, Numerical Study of Heat Transfer Enhancement Due to the Use Of Fractal-Shaped Design for Impingement Cooling, *Thermal Science, 21* (2017), Suppl. 1, pp. S33-S38
[61] Sodjavi, K., *et al.*, Impinging Cross-Shaped Submerged Jet on a Flat Plate: A Comparison of Plane and Hemispherical Orifice Nozzles, *Meccanica, 50* (2015), 12, pp. 2927-2947
[62] Kristiawan, M., *et al.*, Wall Shear Rates and Mass Transfer in Impinging Jets: Comparison of Circular Convergent and Cross-Shaped Orifice Nozzles, *International Journal of Heat and Mass Transfer, 55* (2012), 1-3, pp. 282-293
[63] Sodjavi, K., *et al.*, Passive Control of Wall Shear Stress and Mass Transfer Generated by Submerged Lobed Impinging Jet, *Heat and Mass Transfer, 52* (2016), 5, pp. 925-936
[64] Sodjavi, K., *et al.*, Impinging Jet Passive Control for Wall Shear Stress Enhancement, *Proceedings,* 15th International Heat Transfer Conference, IHTC-15, Kyoto, Japan, 2014, p. 14
[65] Trinh, X. T., *et al.*, Flow and Heat Transfer of Hot Impinging Jets Issuing from Lobed Nozzles, *International Journal of Heat and Fluid Flow, 67* (2017), Oct., pp. 185-201

[66] Frosell, T., Gutmark, E., Dynamics of the Impingement Region of a Circular Turbulent Jet, *Experimental Thermal and Fluid Science*, *91* (2018), Feb., pp. 399-409
[67] Kalifa, R. B., *et al.*, The Effect of Coflows on a Turbulent Jet Impacting on a Plate, *Applied Mathematical Modelling, 40* (2016), 11, pp. 5942-5963
[68] Hansen, L. G., Webb, B. W., Air Jet Impingement Heat Transfer from Modified Surfaces, *International Journal of Heat and Mass Transfer, 36* (1993), 4, pp. 989-997
[69] Chakroun, W. M., *et al.*, Heat Transfer Augmentation for Air Jet Impinged on a Rough Surface, *Applied Thermal Engineering, 18* (1998), 12, pp. 1225-1241
[70] Ekkad, S. V., Kontrovitz, D., Jet Impingement Heat Transfer On Dimpled Target Surfaces, *International Journal of Heat and Fluid Flow, 23* (2002), 1, pp. 22-28
[71] Gau, C., Lee, C. C., Impingement Cooling Flow Structure and Heat Transfer Along Rib-Roughened Walls, *International Journal of Heat and Mass Transfer, 35* (1992), 11, pp. 3009-3020
[72] Gau, C., Lee, I. C., Flow and Impingement Cooling Heat Transfer Along Triangular Rib-Roughened Walls, *International Journal of Heat and Mass Transfer, 43* (2000), 24, pp. 4405-4418
[73] Nakod, P. M., *et al.*, Heat Transfer Augmentation Between Impinging Circular Air Jet and Flat Plate Using Finned Surfaces and Vortex Generators, *Experimental Thermal and Fluid Science, 32* (2008), 5, pp. 1168-1187
[74] Bostanci, H., *et al.*, Spray Cooling with Ammonia on Microstructured Surfaces: Performance Enhancement and Hysteresis Effect, *Journal of Heat Transfer, 131* (2009), 7, pp. 1-9
[75] Silk, E. A., *et al.*, Spray Cooling of Enhanced Surfaces: Impact of Structured Surface Geometry and Spray Axis Inclination, *International Journal of Heat and Mass Transfer, 49* (2006), 25, pp. 4910-4920
[76] Coursey, J. S., *et al.*, Spray Cooling of High Aspect Ratio Open Microchannels, *Journal of Heat Transfer, 129* (2007), 8, pp. 1052-1059
[77] Kim, J. H., *et al.*, Evaporative Spray Cooling Of Plain And Microporous Coated Surfaces, *International Journal of Heat and Mass Transfer, 47* (2004), 14, pp. 3307-3315
[78] Xie, J. L., Study of Heat Transfer Enhancement for Structured Surfaces in Spray Cooling, *Applied Thermal Engineering, 59* (2013), 1-2, pp. 464-472
[79] El-Maghlany Wael, *et al.*, Premium Jet Cooling with Two Ribs Over Flat Plate Utilizing Nanofluid Mixed Convection, *Thermal Science, 21* (2017), 2, pp. 963-976
[80] Zaman, K. B. M. Q., Hussain, A. K. M. F., Vortex Pairing in a cIrcular Jet Under Controlled Excitation. Part 1, General Response, *Journal of Fluid Mechanics, 101* (1980), 3, pp. 449-491
[81] Lai, J. C. S., Turbulence Suppression in an Elliptic Jet, *International Journal of Heat and Fluid Flow*, *13* (1992), 1, pp. 93-96
[82] Ritcey, A., *et al.*, Effect of Jet Oscillation on the Maximum Impingement Plate Skin Friction, *Journal of Fluids Eng.-Transactions of the Asme, 140* (2018), 9, 16
[83] Wiltse, J. M., Glezer, A., Manipulation of Free Shear Flows Using Piezoelectric Actuators, *Journal of Fluid Mechanics, 249* (1993), Apr., pp. 261-285
[84] Parekh, D. E., *et al.*, Innovative Jet Flow Control: Mixing Enhancement Experiments, AIAA Paper 96-0808, 1996
[85] Suzuki, H., *et al.*, Active Control of an Axisymmetric Jet With Distributed Electromagnetic Flaps Actuators, *Experiments in Fluids, 36* (2004), 498-509, pp. 1-43
[86] Davis, M. R., Variable Control of Jet Decay, *AIAA Journal, 20* (1982), 5, pp. 606-609
[87] Denis, S., *Contrôle Du Developpement Des Couches De Mélange Axisymétriques Subsoniques Par Jets Impactant*, Université de Poitiers, 2000, p. 280
[88] Collin, E., *Etude de l'injection radiale de fluide dans une couche de mélange annulaire supersonique*. 2001, Université de Poitiers. p. 282.
[89] Liu, T., Sullivan, J. P., Heat Transfer and Flow Structures in an Excited Circular Impinging Jet, *International Journal of Heat and Mass Transfer, 39* (1996), 17, pp. 3695-3706
[90] Hwang, S. D., Cho, H. H., Effects of Acoustic Excitation Positions on Heat Transfer and Flow in Axisymmetric Impinging Jet: Main Jet Excitation and Shear Layer Excitation, *International Journal of Heat Fluid Flow, 24* (2003), 2, pp. 199-209
[91] Hwang, S. D., *et al.*, Heat Transfer and Flow Structures in Axisymmetric Impinging Jet Controlled by Vortex Pairing, *International Journal of Heat Fluid Flow, 22* (2001), 3, pp. 293-300
[92] Middelberg, G., Herwig, H., Convective Heat Transfer Under Unsteady Impinging Jets: The Effect of the Shape of the Unsteadiness, *Heat Mass Transfer, 45* (2009), Sept., pp. 1519-1532

[93] McGuinn, A., *et al.*, Flow Regime Characterisation of an Impinging Axisymmetric Synthetic Jet. Exp. *Therm. Fluid Sci.*, *47* (2013), May, pp. 241-251
[94] Rylatt, D. I., O'Dovan, T. S., Heat Transfer Enhancement to a Confined Impinging Synthetic Air Jet, *Appl. Therm. Eng.*, *51* (2013), 1-2, pp. 468-475
[95] Sorour, M. M., *et al.*, Experimental Study of Free Single Jet Impingement Utilizing High Concentration SiO_2 Nanoparticles Water Base Nanofluid, *Applied Thermal Engineering, 160* (2019), Sep., pp. 114019
[96] Lai, H. Z., *et al*, An Experimental Investigation of Starting Impinging Jets, *Journal of Fluids Eng.-Transactions of the Asme, 125* (2003), 2, pp. 275-282
[97] Chin, D. T., Tsang, C. H., Mass Transfer to an Impinging Jet Electrode, *Journal of Electrochemical Society*, *125* (1978), 9, 1461
[98] Violato, D., *et al.*, Three-Dimensional Vortex Dynamics and Convective Heat Transfer in Circular and Chevron Impinging Jets, *International Journal of Heat and Fluid Flow, 37* (2012), Oct., pp. 22-36
[99] Selman, J. R., Tobias, C. W., Mass-Transfer Measurements by the Limiting-Current Technique, Advances in Chem. Engng., *Acad. Press, 10* (1978), pp. 211-318
[100]Phares, D. J., *et al.*, The Wall Shear Stress Produced by the Normal Impingement of a Jet on a Flat Surface, *Journal of Fluid Mechanics, 418* (2000), Sept., pp. 351-375
[101]Vallis, E. A., *et al.*, *Techniques of Wall Measurements in Fluid Mechanics*, Euromech, Nancy, France, 1977
[102]Yapici, S., *et al.*, Surface Shear Stress for a Submerged Jet Impingement Using Electrochemical Technique, *Journal of Applied Electrochemistry, 29* (1999), 2, pp. 185-190
[103]Baleras, F., *et al.*, A Three-Segement Electrodiffusion Probe in Axisymmetric Flow with Stagnation and Separation, *Journal of Applied Electrochemistry, 24* (1994), 7, pp. 676-684
[104]Alekseenko, S. V., Markovich, D. M., Electrodiffusion Diagnostics of Wall Shear Stresses in Impinging Jet, *Journal of Applied Electrochemistry, 24* (1994), 7, pp. 626-631
[105]Nastase, I., A. *et al.*, Primary and Secondary Vortical Structures Contribution in the Entrainement of Low Reynolds Number Jet Flows, *Exp. in Fluids, 44* (2008), 6, pp. 1027-1033
[106]El Hassan, M., *et al.*, Experimental Investigation of the Wall Shear Stress in a Circular Impinging Jet, *Physics of Fluids, 25* (2013), 7, 077101
[107]El Hassan, M., *et al.*, Experimental Investigation of the Wall Shear Stress and the Vortex Dynamics in a Circular Impinging Jet, *Experiments in Fluids, 52* (2012), 6, pp. 1475-1489
[108]Sodjavi, K., *et al.*, PIV and Electrodiffusion Diagnostics of Flow Field, Wall Shear Stress and Mass Transfer Beneath Three Round Submerged Impinging Jets, *Experimental Thermal and Fluid Science, 70* (2016), Jan., pp. 417-436

Paper submitted: July 13, 2020
Paper revised: July 20, 2020
Paper accepted: July 21, 2020